Geological Quarterly, 2021, 65: 57
DOI: http://dx.doi.org/10.7306/gq.1626

Chemical and morphological characterization of polymetallic (Mn-Fe) nodules from the Clarion-Clipperton Zone in the Pacific Ocean

Agata KOZŁOWSKA-ROMAN[1, *] and Stanisław Z. MIKULSKI[1]

[1] Polish Geological Institute – National Research Institute, Rakowiecka 4, 00-975 Warszawa, Poland

Kozłowska-Roman, A., Mikulski, S.Z., 2021. Chemical and morphological characterization of polymetallic (Mn-Fe) nodules from the Clarion-Clipperton Zone in the Pacific Ocean. Geological Quarterly, 65: 57, doi: 10.7306/gq.1626

Associate Editor: Tomasz Bajda

Geochemical studies (WD-XRF, ICP-MS, and GF-AAS) have shown that polymetallic nodules from the eastern Clarion-Clipperton Zone (CCZ) in the Pacific Ocean are enriched in several metals such as Cu (mean 1.16%), Ni (1.15%), Co (0.15%), and Zn (0.14%), as well as remarkable contents of Mo (0.059%), V (0.04%), Ce (0.019%), Nd (0.011%), Li (0.015), and Pt (43 ppb). The average content of REE, together with Y and Sc, is 620 ppm. In nodules from the CCZ metal concentrations are often much higher than those reported in nodules from other ocean basins in the world. The bulk-nodule mean value of the Mn/Fe ratio is 5.3, which is characteristic for a mixed (hydrogenetic and diagenetic) origin of the nodules. Microprobe investigation revealed two different chemical compositions of the layers, and ascertained their general metal content. The nodules analyzed are composed mainly of concentric-collomorphic laminae of Mn and Fe (oxy)hydroxides which crystallized around mineral nuclei (e.g., quartz, clay minerals), bioclasts or rock fragments. They are from 3.3 to 7.6 cm in diameter. The chemical and physical properties of the laminae allowed distinction of two genetic types: hydrogenetic and diagenetic. Those formed as a result of hydrogenesis had increased values of Co, Si, Cl and S, while formed diagenetically showed increased levels of Cu, Ni, Mg, Zn and K. These lamina types are characterized by different growth structures, reflectivity, density and Mn/Fe ratios. The ratio of the diagenetic layers to hydrogenetic layers (192/53) in representative polymetallic nodules shows that the nodules of this study are of mixed hydrogenetic-diagenetic type. A mixed genesis was also shown by discriminant diagrams, with these CCZ samples being located at the transition between typical hydrogenetic and diagenetic fields.

Key words: polymetallic nodules, critical elements, rare earth elements, deep-sea mining, Clarion-Clipperton Fracture Zone, Pacific.

INTRODUCTION

One of the most characteristic and prospective occurrences of polymetallic nodules is a vast area in the Eastern Pacific Ocean, located between two fracture zones: Clarion and Clipperton (CCZ; Bonatti et al., 1972; Cronan, 1977; Baturin, 1988; von Stackelberg and Beiersdorf, 1991; Kotliński, 1999; Hein, 2000; Glasby, 2006). Samples of polymetallic nodules from the CCZ, collected during the research cruise of the Inter Ocean Metal (IOM) organization in 2014, were subjected to study at the Polish Geological Institute – National Research Institute, focusing on the chemical and morphological properties of these polymetallic nodules, including bulk geochemical analyses of the nodules for major oxides and for over 40 chemical elements including ones critical to industry. Moreover, the detailed geochemistry of the nodule laminae were investigated by electron microprobe. This study provided new data concerning polymetallic nodules from the CCZ, that we compare with those from other areas within the CCZ zone as well as with data from other parts of the world.

RESEARCH AREA

The research was carried out at PGI-NRI on polymetallic nodules from the IOM organization concession block within the Clarion-Clipperton Zone (CCZ) in the Pacific Ocean (Kotliński, 2011). This area lies on the oceanic abyssal plain at a depth between 4000 and 6000 m, where the rate of sediment accumulation is very low (Depowski et al., 1998; Yubko 2009; Hein and Petersen, 2013). The CCZ is located within the Pacific Plate in the central Pacific Ocean. It is a part of the abyssal plain between Mexico and Hawaii, limited by two large E–W fracture zones – Clarion in the north and Clipperton in the south, and is one of the best-known areas of the Pacific Ocean (Gordon, 2000; Neall, 2008). The CCZ total area is ~5.5 million km^2, extends for ~5200 km from NE to SW, and is ~1000 km wide. Within the zone, many faults intersect each other, with horsts and grabens striking north-south, forming an irregular bottom topography (Kazmin, 2009). The complicated relief of this area, with its main lineaments is shown on Figure 1. The entire area

* Corresponding author, e-mail: agata.kozlowska-roman@pgi.gov.pl

Received: September 20, 2021; accepted: November 12, 2021; first published online: December 20, 2021

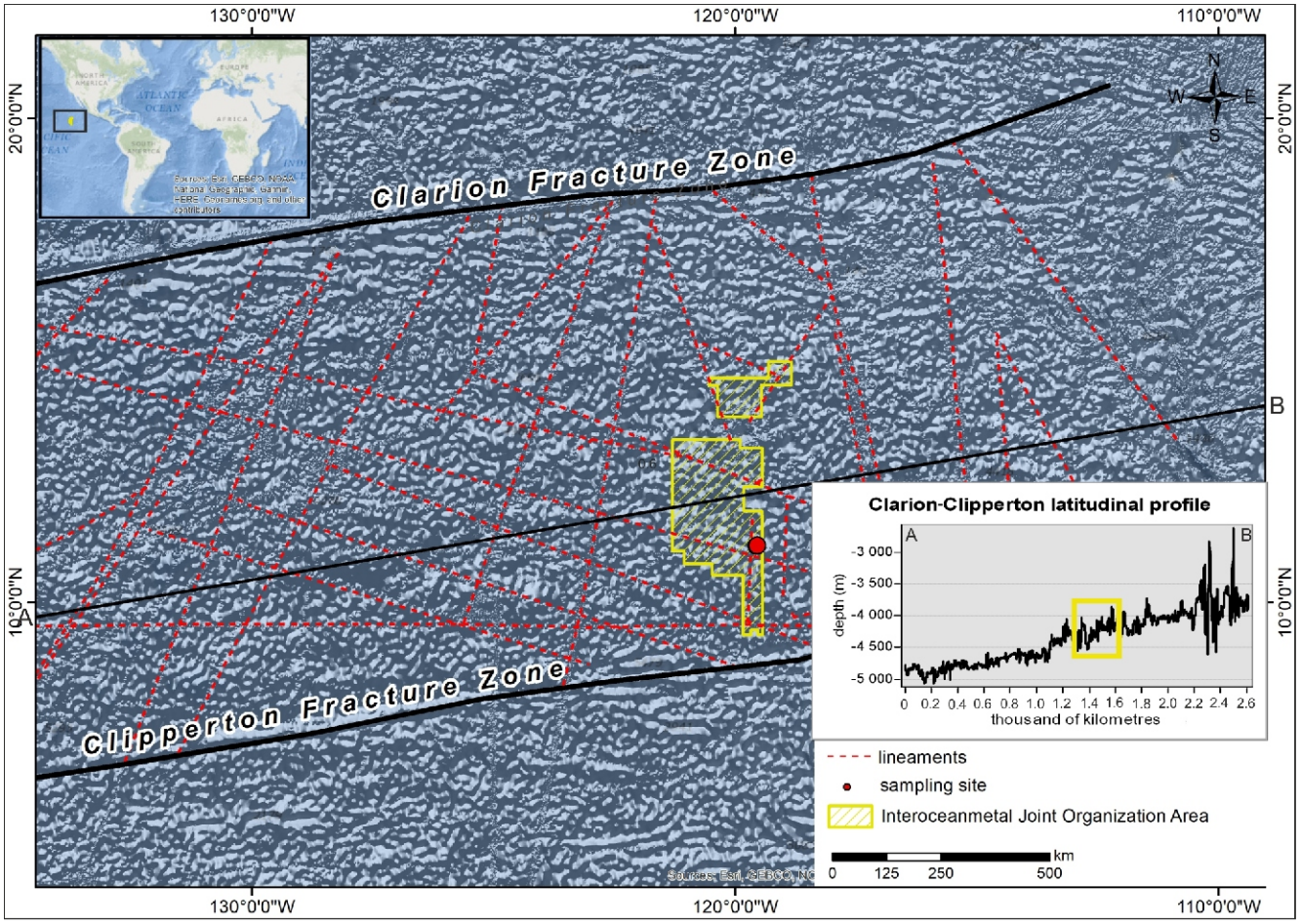

Fig. 1. Map of the sampling site during the research cruise in 2014 in the CCZ with structural tectonic sketch and profile line parallel to the fracture zones (based on the Esri Ocean Basement; bathymetry source – GEBCO)

gradually slopes south-westwards from the Mathematicians palaeorift where the depth is ~3500 m above sea bottom to the Lain volcano-tectonic chain at a depth of 5700 m (Yubko and Kotliński, 2009). The sedimentary cover of the CCZ consists of carbonate-silica deposits of Upper Cretaceous to Quaternary age that gradually thin from west to east (Hein et al., 1997; Usui and Someya, 1997; Kotliński, 2011). Bottom profiling led researchers of the IOM to confirm previous observations regarding bottom morphology (Kotliński, 1992; Yubko, 2009; Ruhlemann et al., 2011). The seafloor is characterized by wide and long NNE–SSW oriented horst and graben structures. Between these, the height differences are from ~100 to 300 m. The distribution of elevations and depressions has a close relationship with the orientation and direction of structural-tectonic zones.

The area considered is characterized by a greater amount of metals delivered into ocean waters from endogenous sources and marked activity of transform faults and ocean fracture zones, which significantly impacts on the geological structure and geomorphology of the CCZ and processes of polymetallic nodule formation (Kotliński and Stoyanova, 2005; Kotliński, 2011, with references therein). It is estimated that the surface coverage is up to ~50% (Rona, 2008).

SAMPLES AND ANALYTICAL METHODS

The material was collected by bottom trawling from a depth of ~4300 m during the IOM-2014 research cruise on the RV "Yuzhmorgeologiya" in 2014. The sampling site of the polymetallic nodules is shown on Figure 1. Chemical analyzes of 10 bulk-nodule samples were carried out at the Chemical Laboratory of the Polish Geological Institute – National Research Institute in Warsaw in 2018. The content of rare earths (Sc, Y, La, Ce, Pr, Nd, Eu, Sm, Gd, Tb, Dy, Ho, Er, Tm, Yb and Lu) and trace elements (Ag, As, Ba, Be, Cd, Co, Cr, Cs, Cu, Li, Mo, Ni, Pb, Rb, Sb, Se, Sn, Sr, Tl, U, V and Zn) were determined after decomposition with a full mixture of HCl, HNO_3, HF, and $HClO_4$ acids using the Perkin Elmer ICP-MS Elan DRC II mass spectrometer utilizing inductively coupled plasma mass spectrometry (ICP-MS).

The major element contents (SiO_2, TiO_2, Al_2O_3, Fe_2O_3, MnO, MgO, CaO, Na_2O, K_2O, P_2O_5, SO_3, Cl and F) and LOI (Loss on Ignition of Solid Combustion Residues) in fused samples from polymetallic nodules were determined. Analyses were performed by wavelength dispersive X-ray fluorescence spectrometry (WD-XRF) method using a *Philips PW-2400* spectrometer. Au, Pd and Pt were measured using the Perkin Elmer

Table 1

Basic statistical parameters of the morphology of the polymetallic nodules studied

Parameter	Arithmetic average	Geometric average	Median	Minimum	Maximum	Standard deviation
Length along the X axis [mm]	55.2	54.7	55.0	33.0	76.0	7.5
Length along the Y axis [mm]	42.6	42.3	43.0	27.0	60.0	5.3
Length along the Z axis [mm]	34.8	34.2	35.0	20.0	60.0	6.5
Volume – V [cm^3]	30.0	28.5	30.0	15.0	72.0	9.6
Weight – W [g]	63.6	60.9	63.9	34.8	130.3	19.1
The ratio of X to Y	1.3	1.3	1.3	0.9	2.2	0.2
The ratio of X to Z	1.6	1.6	1.6	1.0	2.7	0.4
The ratio of Y to Z	1.3	1.2	1.2	0.9	2.0	0.2
The ratio of volume to weight	0.5	0.5	0.5	0.3	1.0	0.1

model 4100 ZL spectrometer by the Graphite Furnace Atomic Absorption Spectrometry (GF AAS) method. The lower limits of detection of these methods are shown in Appendix 1*.

The basic statistical parameters (arithmetic mean, geometric mean, median, standard deviation) of the elemental contents of bulk samples of polymetallic nodules from CCZ were determined, as well as the correlation matrices between elements in the nodules. The degree of correlation of parameters was interpreted as follows: r = 0–0.3 no correlation; r = 0.3–0.5 very weak correlation; r = 0.5–0.7 weak correlation; r = 0.7–0.9 strong correlation; r = >0.9 very strong correlation (Mikulski et al., 2020).

Detailed chemical analysis together with micro-photographic documentation were carried out on 20 thin sections of polymetallic nodules with a *NIKON ECLIPSE LV100 POL* microscope containing *NIS-Elements* software. Quantitative examination of nodules was performed on a *CAMECA SX-100 X-ray* microscope, preceded by preliminary investigation using a *LEO-1430* electron microscope (ZEISS) with an EDS (Energy-Dispersive X-ray Spectroscopy) detector. The following parameters were used during EPMA analyses: HV accelerating voltage 15 kV, beam current 20 nA, focused beam (<1 μm in diameter); acquisition time at peak position 20 s, at background position 10 s, carbon sputtering. The set of elements for quantitative analysis (which was completed on the basis of WDS spectra analysis) is given in Appendix 2. When calculating the chemical composition, the correction for Fe-Ka interference (Mn-Kb1) was taken into account. Values of oxygen concentration (O) were calculated for each element on the basis of its valency, while the share of O for Mn (IV) and Fe (III) (oxidized phases) was calculated.

Using the *ArcGIS* program for working on GIS data and an ocean floor model (*GEBCO 30* arc-second grid), a bottom profile was generated along a line through the CCZ parallel to the fault line. Then, to calculate the average slope of the zone, the depth data was exported from *ArcGIS* to *Excel*, creating another profile, and the trend line was calculated and determined. Using the data generated data and an arctangent function, an average bottom slope of 3.25° to the south-west was obtained (Fig. 1).

RESULTS

MORPHOLOGY OF NODULES

The polymetallic nodules studied mostly have a discoidal, ellipsoidal or spheroidal shape. The longest axis varies from 3.3 to 7.6 cm (Table 1), whereas nodules between 3 and 5 cm are most common. During the research >100 polymetallic nodules were measured and described. From these morphometric parameters, nodule diameter was adopted as the basic criterion for their subdivision. Three groups of nodules were distinguished: (1) small (symbol S) with a diameter of 3.3–4 cm, (2) medium (symbol M) with a diameter of >4–6 cm, (3) large (symbol L) with diameter >6–7.6 cm.

Based on these measurements, it was determined that the average-size nodule is 5.4 cm long (x), 4.2 cm wide (y) and 3.4 cm thick (z) (Table 1). The size relations of the y to x axis and the x to z axis are shown by graphs (Fig. 2A, B). The ratio of length to width is 0.76 and width to thickness 0.62. A slight correlation between nodule length and weight was also noted (R^2 = 0.18; Fig. 2C), as well as a strong correlation between weight and volume R^2 = 0.73 (Fig. 2D).

The average apparent density of polymetallic nodules is between 1.00 and 2.40 g/cm^3 and the porosity is between 25 and 61%. The hardness determined on the basis of the Mohs scale is ~2.5. These values are variable and depend on the size of the nodules. Polymetallic nodules are built mainly of concentric laminae, the growth of which began on a foreign body that is the nodule nucleus. This nucleus may be a mineral grain, fragment of bone (Fig. 3A), particle of sediment, submarine volcanic rock including pumice (Fig. 3B), microorganism (e.g., foraminifer test), or shark tooth (Fig. 3C; Depowski et al., 1998; Kozłowska-Roman and Mikulski, 2019). Often there is more than one nucleus in one polymetallic nodule or new laminae began to build up on broken nodules, as can be seen in thin section.

Large nodules (from 6 to 7.6 cm in size) usually have an irregular shape and discoidal form with relatively fragile structure. The outer surface often looks like spherical clusters or

* Supplementary data associated with this article can be found, in the online version, at doi: 10.7306/gq.1626

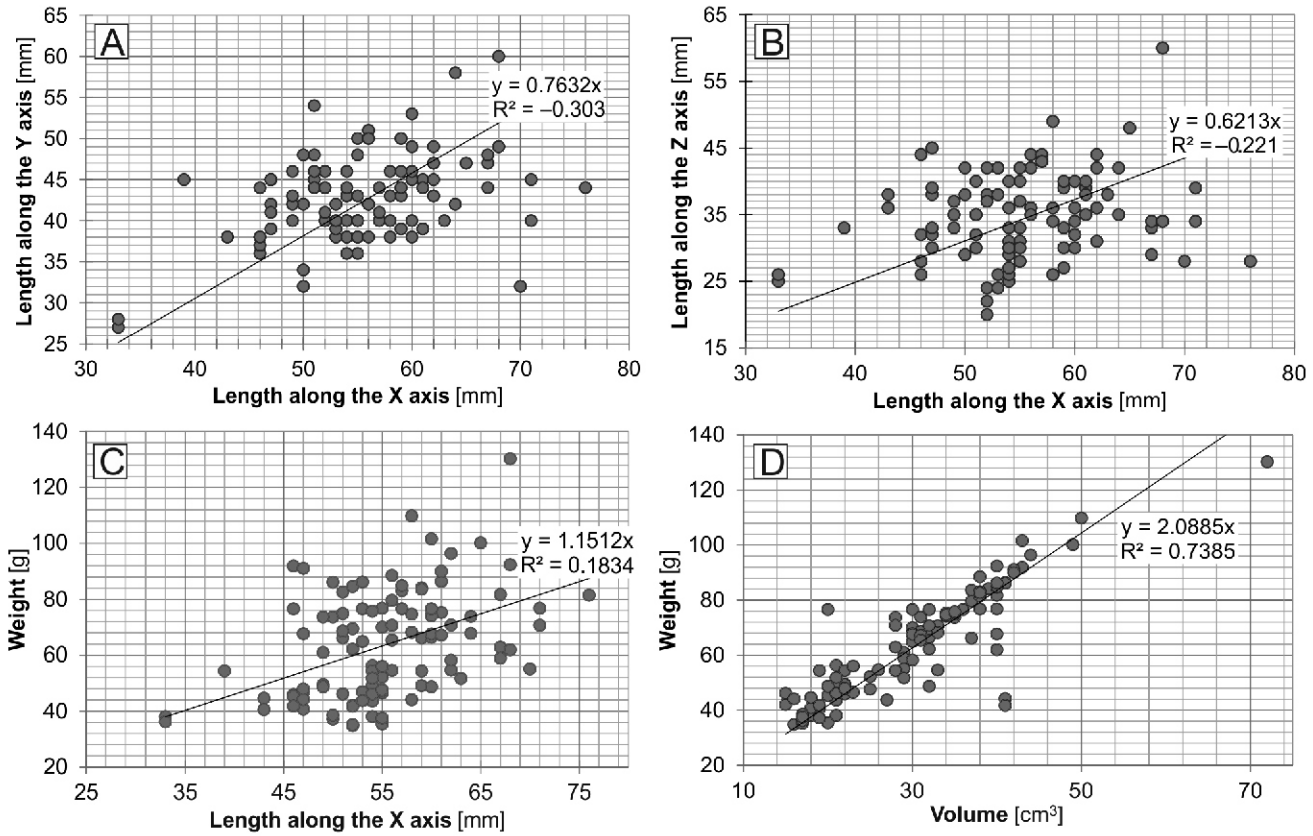

Fig. 2. Graphs of morphological parameters for polymetallic nodules from the CCZ in the Pacific Ocean

A – relation between the length along the X axis and the length along the Y axis [mm]; **B** – relation between the length along the X axis and the length along the Z axis [mm]; **C** – relation between the length along the X axis [mm] and the weight [g]; **D** – relation between volume [cm^3] and weight [g]

crusts (Fig. 4A), from the merger of several nodules and so with more than one nucleus. Because of numerous pores and a very loose structure, sediments fill every open space on the nodule surface and in the more compact internal part (Fig. 4J). Medium nodules (from 4 to 6 cm across) have a discoidal or ellipsoidal form. At the water-sediment interface, a characteristic rim is visible (Fig. 4B). Usually the upper part, where growth took place in direct contact with water, is smooth (Fig. 4D); the lower surface is strongly irregular and often filled with sediment (Fig. 4E). The nuclei of both medium and large examples are commonly fragments of other nodules (Fig. 4F). Small nodules (3.3–4 cm in diameter), with a spheroidal shape and a smooth surface, are more solid and less fragile (Fig. 4G, I). The outer layer is very compact and less porous than in the case of larger nodules, so there is no visible sediment filling the pores in its structure (Fig. 4H). Thin alternating dark and light grey layers are very visible and build out from a central point (Fig. 4C).

BULK SAMPLE GEOCHEMISTRY

Ten selected, well-preserved, dense polymetallic nodules of different sizes (long axis range between 3.3 and 7.6 cm) were analyzed. They have a discoidal to ellipsoidal shape, usually with smooth upper surface and coarse bottom parts. The chemical composition of the polymetallic nodules is dominated share by the following major oxides: MnO (arithmetic mean = 37.1%; n = 10), SiO_2 (12.8%), Fe_2O_3 (7.8%), Al_2O_3 (4.3%), MgO (2.8%), Na_2O (2.8%), CaO (2.2%) and others with mean content <0.1% (Table 2 and Fig. 5). The range of variability of their composition for individual oxides is small and ranges from 0.06% (SO_3) to 3.67% (MnO), depending on the oxide. In general no significant differences in the major oxides geochemical composition between nodules of different size were found. Manganese (MnO) concentration is from 35.82 to 39.49% and iron (Fe_2O_3) from 6.35 to 8.75%. The mean Mn/Fe ratios in bulk nodule samples is 5.3 and ranges from 4.6 to 6.9. Some of the larger nodules have slightly higher Mn/Fe ratios (5.3–6.9) as well as Th/U ratios (3.1–4.1) compared to the smaller ones (Mn/Fe 4.8–5.5 and Th/U 2.5–2.7; Appendix 3). MnO and SiO_2 constitute on average >50% of the nodule, and the remaining oxides average ~22%. The Si/Al ratio is between 2.46 and 2.77 with a mean of 2.64, generally <3 indicating the presence of clay minerals within the nodules. The large share of LOI values (range from 23.1 to 24.8 wt.%) is due to the primary water and volatile content lost during sample drying and chemical analyses.

These nodules consist mainly of Mn and Fe, and additionally of Cu (arithmetic mean = 1.16%), Ni (1.15%) and Co and Zn (1521.7 and 1439.0 ppm, respectively), as well as prominent contents of Mo (590.6 ppm), V (412.8 ppm), Ce (192.4 ppm), Li (157 ppm), Nd (114.3 ppm) and Pt (43.1 ppb). The metal content of the nodules, excluding Fe and Mn, is on average ~3% (Fig. 5), the highest being Cu (1.22% of the total average mass of the sample), Ni (1.20%), Ba (0.24%), Co (0.16%), Zn (0.15%), Mo (0.06%), REE (0.06%), V (0.04%), Li (0.2%) and other metals (0.2% each). The smaller nodules have a slightly

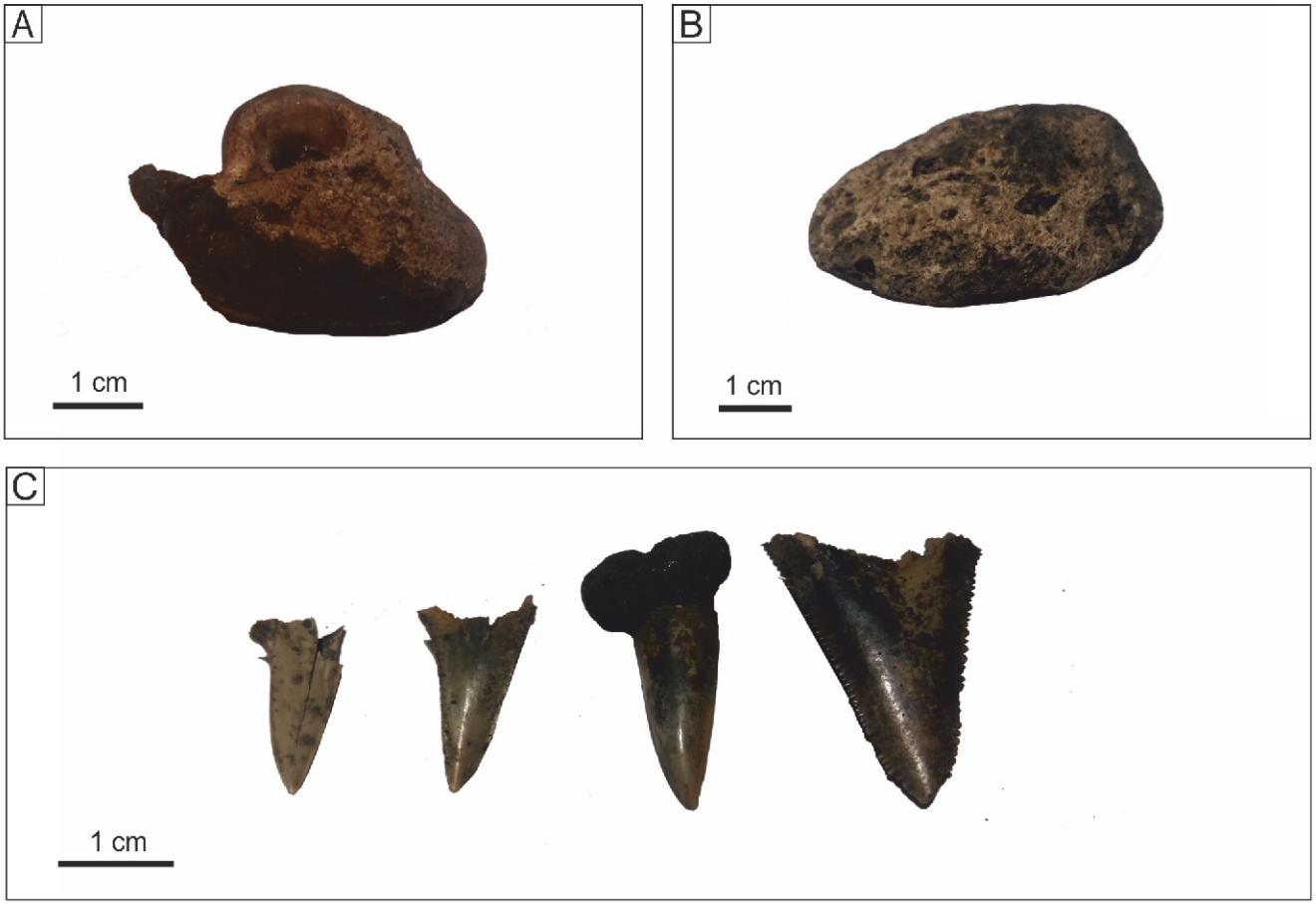

Fig. 3. Examples of nodule nuclei from the study area

A – fragment of bone; **B** – pumice; **C** – shark tooth (*Lamniformes*: Lower Cretaceous–present)

higher Co+Cu+Ni concentration (2.5–2.7%) compared to the bigger ones (2.3–2.5%; Appendix 3). There is a strong negative correlation between MnO and Fe_2O_3 (correlation coefficient, r = –0.82). A very strong correlation (r 0.9) between Cu and CaO, Zn, and Na_2O concentrations was found (Appendix 4). A strong correlation (r = 0.9–0.7) exists between the distribution of Cu and Mo, Sb, Zn and Au, Ni and As, U, Mo, CaO and P_2O_5, Fe_2O_3 and As, P_2O_5, and Sr as well as between Co and SiO_2 and K_2O, Zn and Au, CaO, Mo, and Cd. Moreover, a strong correlation was recognized between the content of Mo and CaO, As and Tl, Be and As and Ag, Sb and Cd, and Au, Li, and Na_2O. Weak correlations (r = 0.7–0.5) were found between some major oxides and/or major and minor element distributions. Mn/Fe ratios have a weak correlation with MgO distribution (r = 0.55), but negative strong correlation with As, P_2O_5, Sr and Be. The sum of Cu+Co+Ni shows a very strong correlation with CaO and Cu distribution and a strong correlation with Mo, Ni, Au, As and Zn but strong negative correlation with MgO. The largest changes in the value of the standard deviation coefficient from the arithmetic mean value for the elements and oxides examined were found for: Pt, Au, Pd (from 50–60%), Se, SO_3, Ba, Tl, Ag (from 30–40%), Sn, CaO, Li, K_2O, As, Cr, Cd, Cs, Sc and Th (from 10–20%). The lowest values of changes in the standard deviation in relation to the average value of a given element or oxide were found for MnO and Ni (2.8 and 3.9%, respectively). For other determinations of elements, the content ranges from ~5 to 10%.

Figure 6 shows a comparison of the element contents of polymetallic nodules from the CCZ to their average crustal abundance (Barbalance, 2019). A very strong enrichment in Mo (almost 400x), Mn (300x), Sb, Cu and Tl (200x) are evident. The contents of Cd and Ni show over 100x enrichment. In turn Co and Se show an increase of 70x and 60x, respectively. Arsenic shows almost 40 times the enrichment and elements such as Zn, Pd, Pb, Pt and Ag over 10 times the enrichment compared to their average content in the Earth's crust. Be, Cr, Rb, Sc and Sn are depleted elements with respect to the crustal mean composition by a factor of between 5 and 10.

The bulk average content of the sum of REE together with Y and Sc (i.e. REY) for polymetallic nodules is ~618.3 ppm (n = 10 samples; range from 561.9 to 687.8 ppm). The average REY content is 608.8 ppm and ranges from 553.6 to 677.4 ppm. The average REY contents in nodules from the study area is in the range of the REY contents in nodules from other parts of the CCZ in the Pacific Ocean (average = 762.1 ppm; range from 400 to 1040 ppm), (Glasby, 1977; Kotliński et al., 1997; Hein et al., 2013; Hein and Koschinsky, 2014). Analysis of the chemical composition of 158 polymetallic nodules from the CCZ showed that REE is in the range from 302 to 2020 ppm (Kotliński et al., 1997; Duliu et al., 2009; Franzen and Balaz, 2012; Dimitrina et al., 2014; Zawadzki et al., 2015). But it is significantly lower than that in polymetallic nodules found in the Cook Island Exclusive Economic Zone in the Pacific Ocean (REY average contents = 0.168%, max.

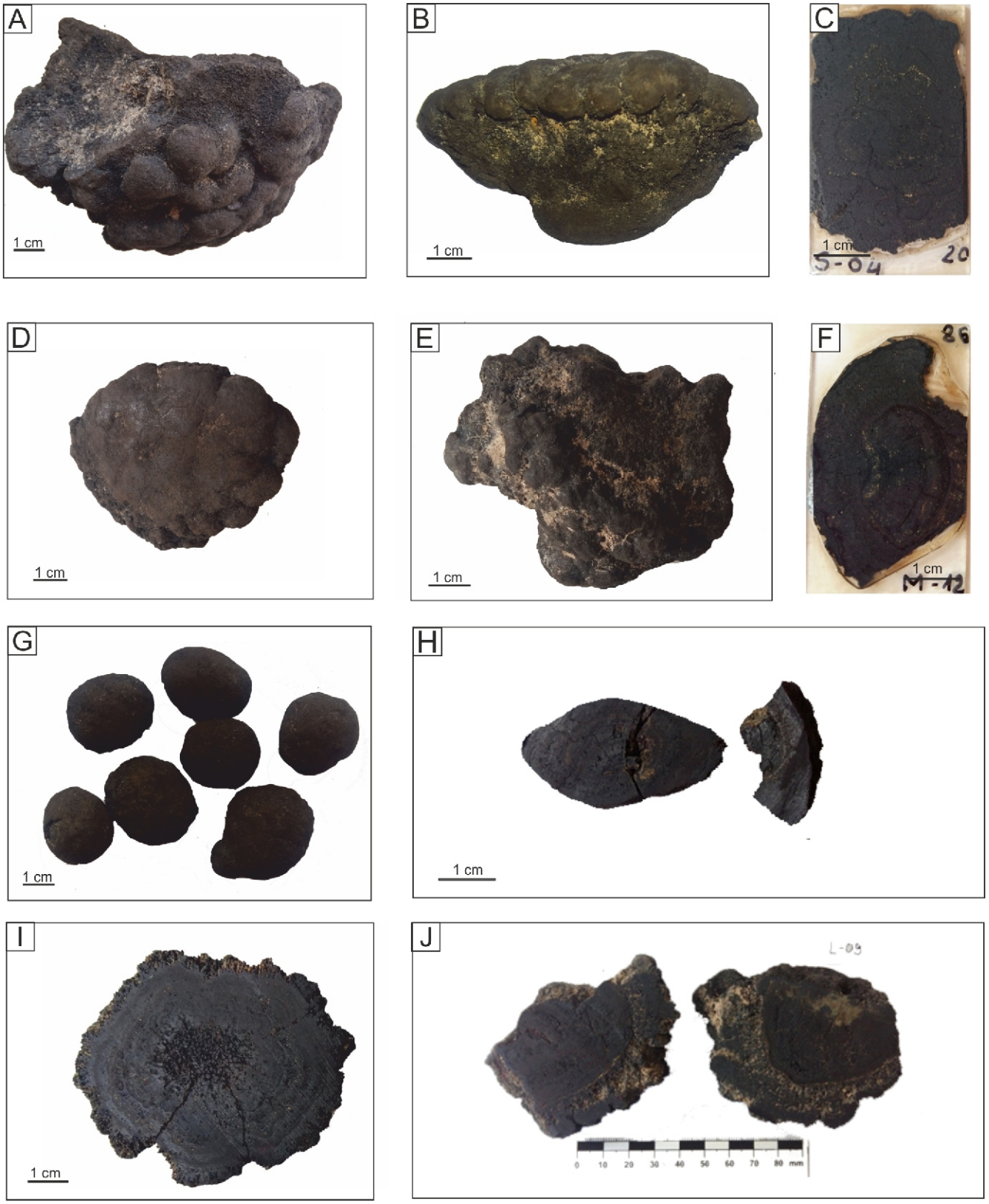

Fig. 4. Typical polymetallic nodules from the CCZ in the Pacific Ocean

A – large polymetallic nodule with convex surface, weight 203 g, size 7.6x5.5x5 cm; **B** – polymetallic nodule with a visible rim marking the water-sediment interface; **C** – thin section of small polymetallic nodule; **D** – polymetallic nodule formed by the precipitation of metal ions from bottom waters; **E** – rough surface of a nodule formed by the precipitation of metal ions from pore waters in the sediment; **F** – thin section of medium polymetallic nodule with a nucleus in the form of a fragment of another nodule; **G** – small polymetallic nodules with a smooth surface; **H** – cross-section through small polymetallic nodule; **I** – cross-section through medium polymetallic nodule; **J** – cross-section through large polymetallic nodule with sediment visible in numerous pores

Table 2

Basic statistical parameters for main oxides and major and trace elements from geochemical bulk-rock analyses of polymetallic nodules from the CCZ in the Pacific Ocean

Component	Arithmetic mean	Geometric mean	Median	Minimum	Maximum	Standard deviation
MnO [%]	37.06	37.04	36.73	35.82	39.49	1.05
SiO_2	12.82	12.81	12.81	12.24	13.70	0.45
Fe_2O_3	7.81	7.78	7.90	6.35	8.75	0.72
Al_2O_3	4.29	4.29	4.25	4.05	4.65	0.21
MgO	2.84	2.83	2.88	2.61	3.18	0.18
Na_2O	2.78	2.78	2.84	2.60	2.98	0.14
CaO	2.15	2.13	2.08	1.75	3.15	0.38
K_2O	0.82	0.81	0.85	0.67	0.94	0.10
TiO_2	0.35	0.35	0.34	0.31	0.41	0.032
SO_3	0.44	0.42	0.38	0.29	0.88	0.18
P_2O_5	0.29	0.29	0.29	0.25	0.31	0.02
Cl	0.08	0.08	0.07	0.06	0.09	0.01
LOI	23.99	23.98	23.85	23.10	24.80	0.53
SUM [%]	95.50	95.50	95.56	95.02	95.73	0.22
Li [ppm]	156.98	155.00	159.05	118.00	203.30	26.32
Be	1.59	1.58	1.57	1.26	1.78	0.17
V	412.8	412.4	412.0	381.0	447.0	18.7
Cr	8.3	8.25	8.0	7.0	10.0	0.95
Co	1521.7	1517.6	1526.0	1297.0	1711.0	115.9
Ni	11502.1	11494.2	11503.0	10745.0	12210.0	447.2
Cu	11628.7	11607.9	11319.5	11196.0	13599.0	760.9
Zn	1439.0	1433.5	1452.0	1263.0	1683.0	133.4
As	57.7	57.3	58.0	43.0	65.0	6.6
Se	3.1	2.8	3.5	1.0	5.0	1.2
Rb	22.4	22.3	22.8	19.6	24.5	1.7
Sr	609.6	608.8	610.6	549.0	680.8	33.5
Mo	590.6	589.1	589.5	517.8	672.4	44.0
Ag	0.99	0.91	1.17	0.27	1.32	0.35
Cd	20.94	20.79	20.72	15.70	24.00	2.57
Sn	0.93	0.91	1.00	0.50	1.10	0.21
Sb	51.7	51.6	51.9	45.9	60.7	4.1
Cs	1.57	1.56	1.57	1.33	1.94	0.19
Ba	2303.7	2161.7	1933.5	1472.0	3965.0	917.1
Tl	129.7	122.6	138.9	61.6	181.1	40.59
Pb	219.0	218.2	217.0	192.7	251.3	19.9
U	3.37	3.36	3.37	3.13	3.63	0.19
Sc	9.55	9.50	9.65	8.30	10.80	0.96
Y	68.84	68.77	69.00	63.40	75.20	3.11
La	86.42	86.32	86.53	78.20	94.00	4.25
Ce	192.40	191.86	192.48	170.10	216.90	15.25
Pr	26.86	26.81	26.90	23.80	29.90	1.56
Nd	114.27	114.10	114.60	104.00	128.80	6.45
Sm	28.06	28.02	28.07	25.58	31.48	1.58
Eu	7.21	7.19	7.14	6.39	8.32	0.49
Gd	26.78	26.75	26.73	24.63	29.58	1.33
Tb	4.15	4.14	4.13	3.70	4.62	0.24
Dy	23.53	23.50	23.45	20.99	26.35	1.38
Ho	4.33	4.32	4.33	3.93	4.82	0.23
Er	11.84	11.82	11.88	10.73	13.21	0.67
Tm	1.66	1.66	1.65	1.49	1.86	0.10
Yb	10.84	10.82	10.79	9.70	12.17	0.66
Lu	1.61	1.61	1.62	1.45	1.81	0.1
Th	11.19	11.11	10.76	9.23	14.10	1.39

Tabl. 2 cont.

Au [ppb]	1.45	1.20	1.50	0.50	3.00	0.86
Pt [ppb]	43.10	34.07	38.00	5.00	96.00	26.31
Pd [ppb]	11.10	9.25	12.00	2.50	18.00	5.50
REE(La-Lu)+Y+Sc	618.3	617.4	618.9	561.9	687.8	33.38
REE [ppm] (La-Lu)	539.9	539.1	540.1	490.2	602.2	32.2
SLREE (La-Eu)	455.2	454.4	455.6	413.6	507.8	26.43
SHREE (Gd-Lu)	84.7	84.6	84.5	76.6	94.4	4.65
REY (La-Lu+Y)	608.8	607.9	609.7	553.6	677.4	34.85
HREY (Gd-Lu+Y)	153.6	153.4	154.1	140.0	169.6	7.58
LREE/HREE	5.37	5.37	5.39	5.14	5.61	0.12
LREE/HREY	2.96	2.96	2.97	2.78	3.10	0.08
Mn/Fe	5.31	5.28	5.25	4.60	6.89	0.677
Co+Cu+Ni [%]	2.47	2.46	2.44	2.34	2.71	0.102
Si/Al	2.64	2.64	2.66	2.46	2.77	0.10
Th/U	3.33	3.31	3.31	2.83	4.12	0.402

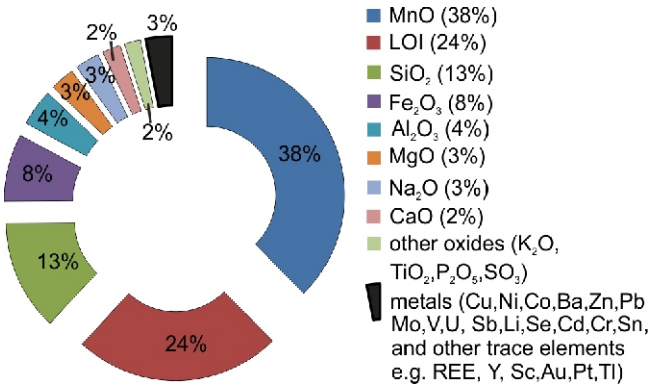

Fig. 5. Ring diagram of the bulk-rock sample chemical composition (in wt.% calculated to 100%) of polymetallic nodules from the CCZ in the Pacific Ocean

0.321%; Hein et al., 2015). They are also lower than in the Indian Ocean polymetallic nodules where the average REY content is 0.104% (Hein and Koschinsky, 2014). Moreover, comparing the mean content of REY to their mean content in siliceous-clayey silts reported by Zawadzki et al. (2020) from the eastern parts of the CCZ, a more than doubled enrichment should be found (average REY = 288.81 ppm for n = 137, range from 199.99 to 616.56 ppm). The nodules studied also show higher mean REY concentrations compared to polymetallic nodules from the Peru Basin in the Pacific Ocean, in which the average REY contents are 402.51 ppm (Hein and Koschinsky, 2014). They are also almost 4x higher than the average concentrations of REY – 165.1 ppm, LREE (145.7 ppm) and HREE (19.4 ppm) recorded for Fe-Mn nodules from the southern part of the Baltic Sea in the Polish Maritime Areas (Szamałek et al., 2018). REE have a strong correlation (r = 0.88–0.81) with TiO_2, Pb, Y and Th. Kotlinski et al. (1997) suggested that REE are fixed to nonmetalliferous accessoric min-

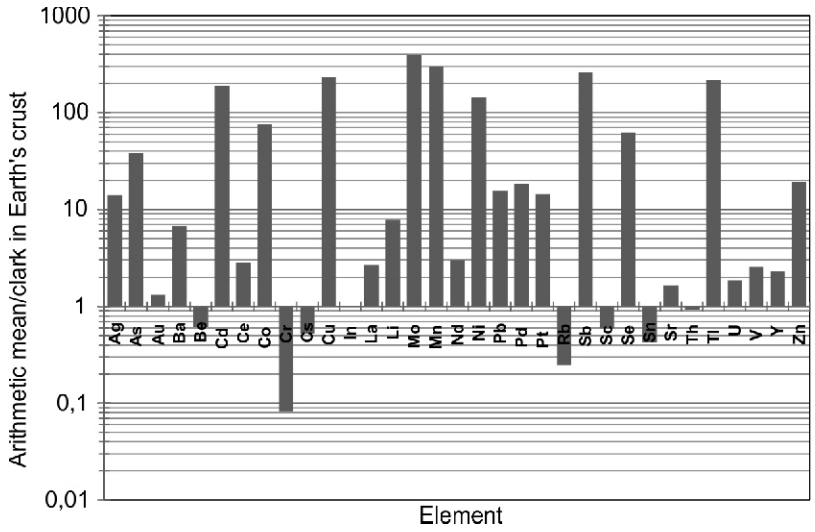

Fig. 6. Comparison of the arithmetic mean content of some elements in bulk-rock samples of polymetallic nodules from the CCZ in the Pacific Ocean relative to their average contents in the Earth's crust (after Barbalance, 2019)

Elements above the ratio line of 1 are enriched in the nodules

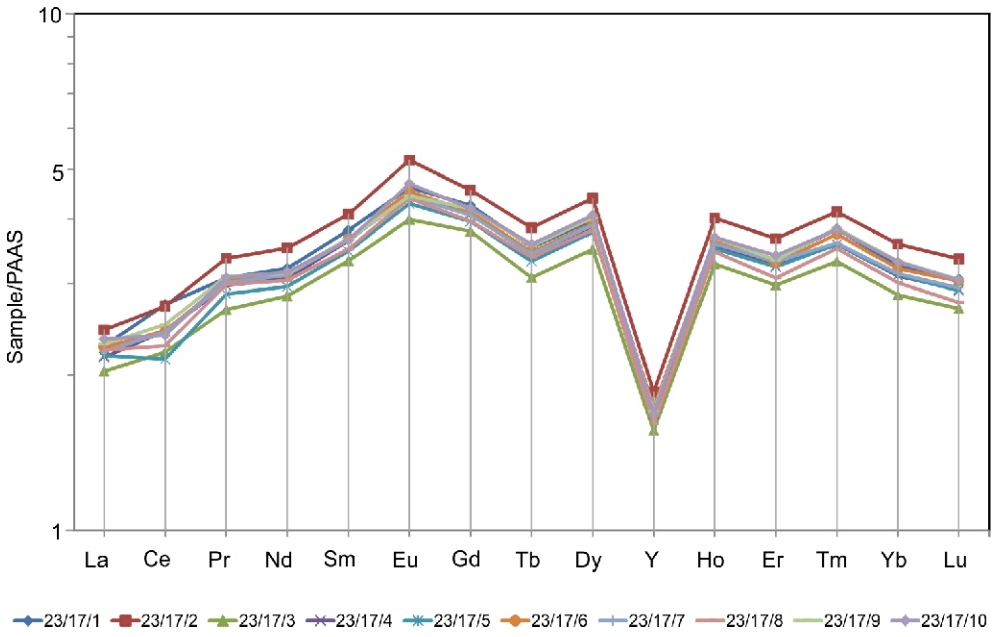

Fig. 7. REE diagrams normalized to PAAS (after McLennan, 1989) of polymetallic nodules from the CCZ in the Pacific Ocean

erals such as barite, mica, feldspar and other. In concretions from the CCZ zone, hydrogenetic nodules show higher average REE concentrations (1065 ppm) than the diagenetic nodules (787.9 ppm; Zawadzki et al., 2015). We found that the mean sum of REE (La-Lu) is 539.9 ppm (range 490.2–602.2 ppm), which is almost 2x lower than the reported mean values for hydrogenetic concretions and over 230 ppm lower than for diagenetic concretions; the small nodules contain lower REE than with the largest ones.

REY data ploted relative to Post Archean Australian Shale (PAAS; McLennan, 1989) are characterized by an increased concentration of LREE compared to HREE and a positive europium anomaly and negative yttrium anomaly (Fig. 7). The REE pattern also shows slight Tb and Er negative anomalies. PAAS-normalized Eu anomalies show positive enrichments ranging from ~5 to 11 and significant negative Y anomalies ranging from 1.5 to 1.8. The arithmetic mean value of the LREE/HREY ratio is 2.96 (ranges from 2.8 to 3.1).

NODULE GEOCHEMISTRY IN THE LIGHT OF MICROPROBE STUDIES (EPMA)

In mineralogical terms, the polymetallic nodules investigated consist of Mn oxides and Fe hydroxides. The main manganese minerals within the nodules analyzed are low-crystalline vernandite, todorokite, birnesite and polymorphic iron hydroxide (Hein, 2000; Wegorzewski et al., 2015). Identification of these minerals was possible using X-ray diffraction (XRD), which was not the subject of this study. Instead, EPMA was performed to define macroscopically visible differences in the zoned structure of the nodules (Fig. 8A–F). The macroscopic studies as well as electron microprobe imaging and scanning electron microscopy (SEM) revealed an internal structure characteristic of polymetallic nodules. All methods showed that from the centre of the nucleus or nuclei minerals grow symmetrically forming different types of layers that can be initially distinguished into lighter and darker ones (Fig. 8A–C). In fact they differ in shape, thickness and reflectivity, which is indicative of different metal contents.

The light layers are characterized by high reflectivity which may indicate a higher metal content. Investigations of chemical composition in single layers with the use of EPMA showed that they contain high values of Mn, on average 44.81% (manganese oxide MnO_2 71–79% wt.%) and low iron content, on average 0.86 wt.% (Fe_2O_3 content does not exceed 3 wt.%). The Mn/Fe ratio ranges from 5.5 to 1148.8 and the concentration of Ni+Cu is relatively high and reaches 6.43 wt.% whereas copper oxide is~3 wt.% in the form of CuO, and nickel oxide ~4 wt.% in the form of NiO. In the light laminae the sum values are in average 94.37 wt.% (Table 3, Appendicies 5 and 6). Laminae can also be distinguished by the shape of their growth. Layers with high reflective ability are thicker and wider then dark layers. They usually grow in dendritic forms or are dense and massive. Dendritic forms consist of sections of locally thickened laminae. They are dense and rounded (Fig. 8A). This type of layer is very common and covers a large area of the inner nodule structure. Massive in structure, dense and thick, they often contain many fragments of microfauna such as radiolaria and diatoms, which may have grown within the sedimentary pore space (Fig. 8B).

The dark layers with low reflectivity contain significant amounts of iron in the range of 5.7–17.9 wt.% and an increased content of silicon, on average 3.93 wt.%, compared to light laminae. The Mn/Fe ratio ranges from 1 to 5 and the concentration of Ni+Cu is relatively low at up to 3.43 wt.% whereas copper oxide in the form of CuO and nickel oxide in the form of NiO is ~1 wt.%. Measurements of the chemical composition in laminae on the microprobe showed significantly lower analytical sums, on average 83.36 wt.%. In general, the analytical sums of the EPMA measurements are often <100 wt.% because of the high porosity of the nodule structures and the high amounts of water within the crystal structure of the different oxides (Table 3, Appendicies 5 and 6). The dark layers usually grow as fine laminae (Fig. 8C) but also in a dendritic form, often creating an mixed sequence of layers alternating with light layers (Fig. 8D), or they appear as the last porous layer in a sequence of light laminae (Fig. 8E).

Within these layers, irregular porous areas occur with components such as feldspar, barite, ilmenite, pyroxene as deter-

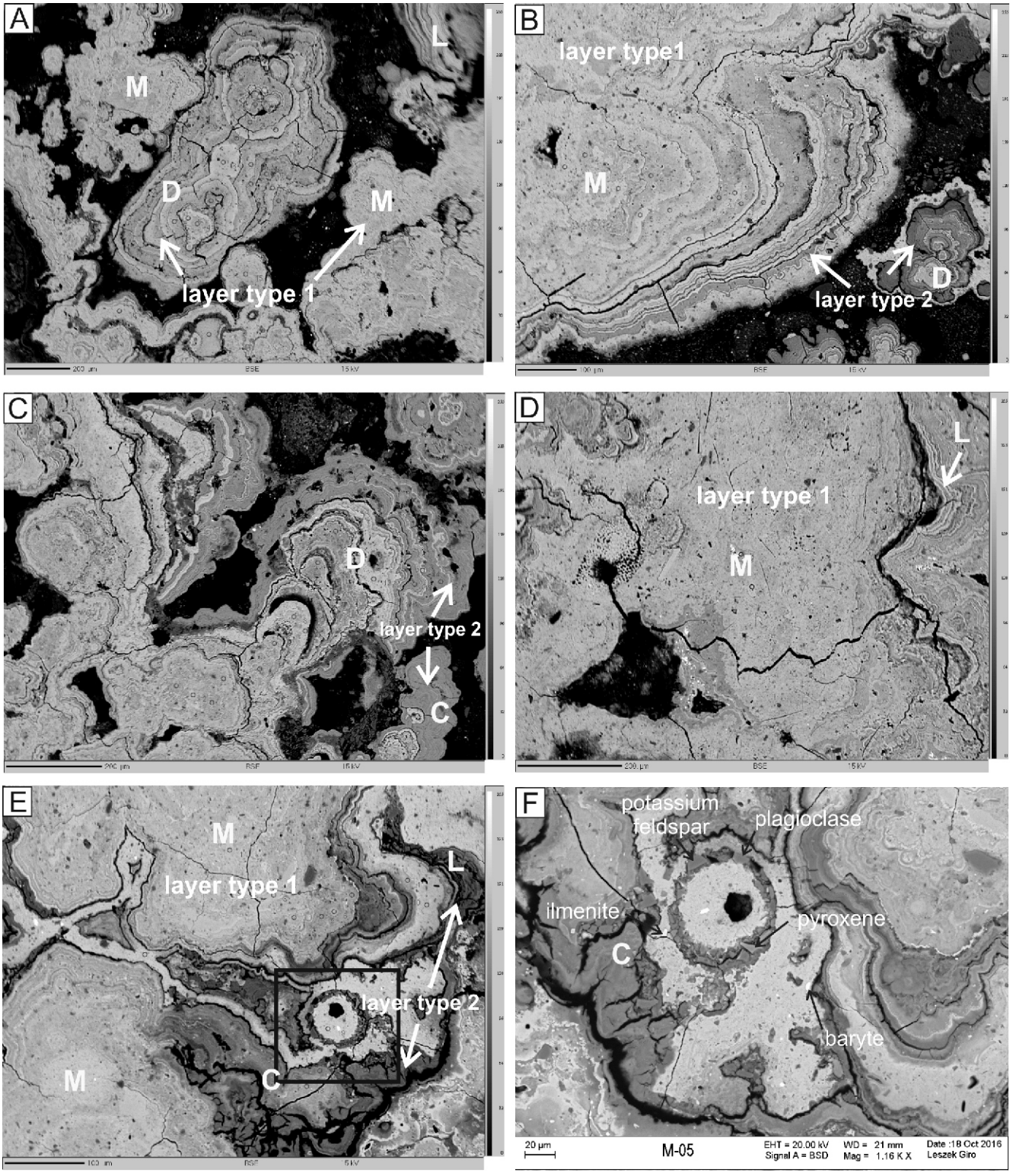

Fig. 8. BSE image of internal structures in the polymetallic nodules, with layers of high and low reflectivity indicating changes in Mn/Fe ratios

A – example of dendritic growth structure (D) and massive structure (M) in high-reflectivity layer; **B** – massive structure containing numerous fragments of microfauna such as radiolaria and diatoms; **C** – example of finely layered growth structures (L) in low-reflectivity layer; **D** – dendritic form in mixed sequence of alternating dark and light layers and columnar growth in a low reflectivity layer; **E** – example of layers with dendritic growth structures and columnar growth (C) forming microscopic cauliflower-shaped structures; **F** – scanning electron microscope image of a porous area containing components such as feldspar, barite, ilmenite and pyroxene (rectangle in Fig. 8C)

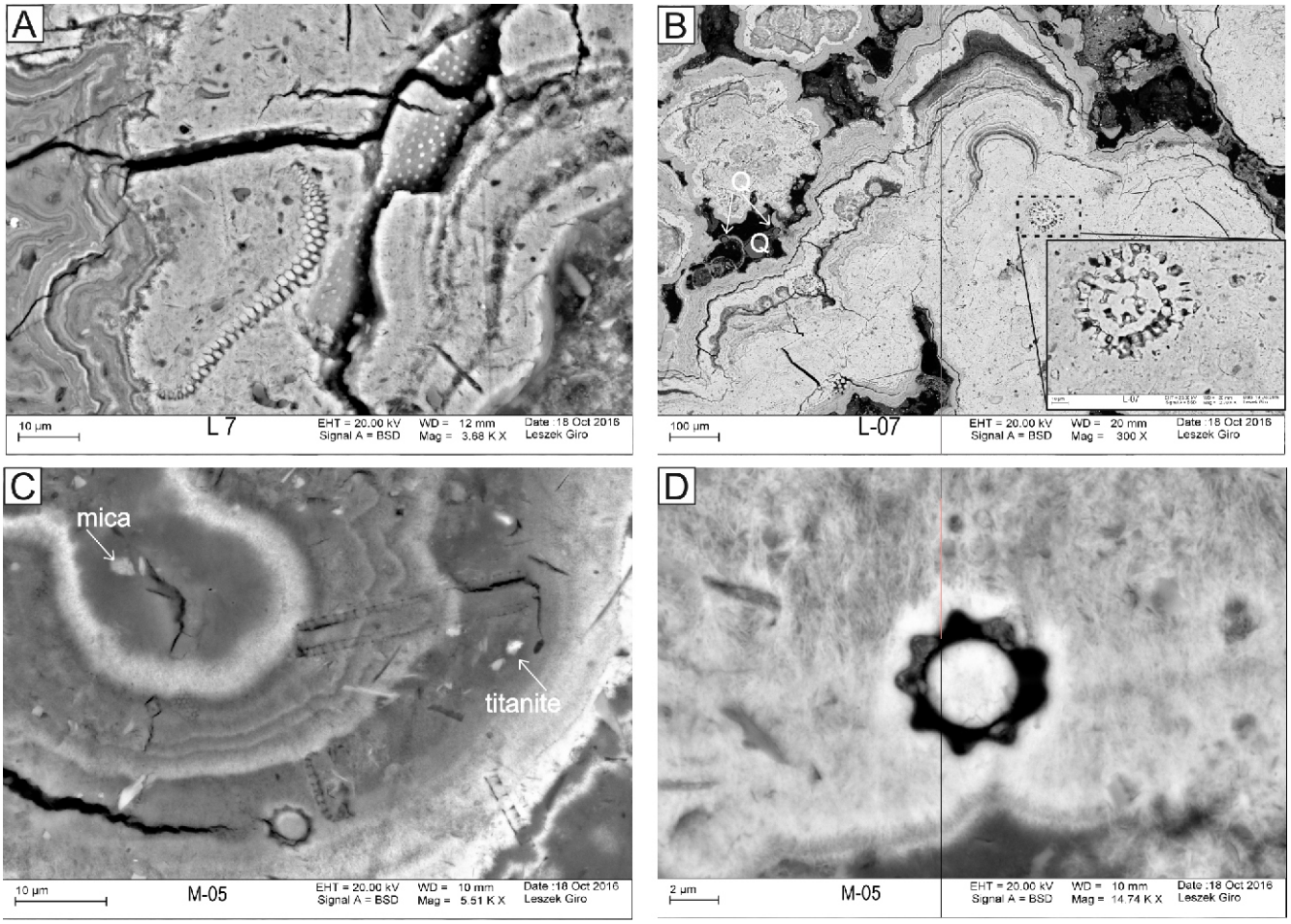

Fig. 9. Image of scanning electron microscope (SEM) with microfauna and mineral grains within a polymetallic nodule

A – fragment of radiolarian within high-reflectivity massive layer; **B** – radiolarian mould and quartz grains; **C** – cross-section through the middle part of a polymetallic nodule rich in microorganisms and mineral grains of titanite and mica, the microfauna does not significantly disturb the growth of the new layers; **D** – section through radiolaria

mined by the EDX analysis (Fig. 8F). The internal structure of nodules also includes microfossil fragments such as diatoms and radiolaria, replaced by Mn (Fig. 9A, B, D). In many SEM images the microorganisms present do not interfere with the growth of subsequent nodule layers (Fig. 9C).

DISCUSSION

In these studies of nodules from the IOM organization concession block within the eastern part of the CCZ in the Pacific Ocean, their bulk-rock chemical composition was determined using by ICP-MS, WD-XRF and GFAAS. Additionally, electron microprobe (EPMA) and scanning microscopy (SEM) studies allowed the point chemical composition of individual layers in nodules to be determined. The comparison of bulk chemical analyses of whole samples with the EPMA results shows a very large differentiation of the chemical composition between the bulk-nodule results and individual laminae in nodules. These CCZ nodules have high contents of metals such as Cu, Mo, Ni, Co, Zn and REE. The bulk-nodule average contents of Cu and Ni are very similar, amounting to ~1.1% and they are characteristic of CCZ, and similar to those of Indian Ocean, nodules (1.04% Cu and 1.1% Ni, respectively; Jauhari and Pattan, 2000; Hein et al., 2013; Mukhopadhyay et al., 2018). In turn, the contents of Cu and Co in the CCZ are much higher than, for example, for the Peru Basin (mean = 0.59% Cu, mean = 0.0475% Co; Hein et al., 2013). Average cobalt concentrations in the CCZ (= 0.15%) are similar or slightly lower than those reported for the North-East Pacific Basin. For example, Hein et al. (2013) for nodules from the CCZ gives a mean value of 0.2098% Co, and Kotliński (1999) for CCZ of 0.214% Co, for the California Basin of 0.136% Co, and for the Hawaian Basin of 0.557% Co. On the other hand, the mean concentrations of Mn in the nodules studied (28.7%) are similar to or slightly higher than the content reported by other authors for nodules from other parts of CCZ (e.g. 28.4% Mn; Hein et al., 2013) or the Indian Ocean (24.4% Mn), but much lower than in nodules from the Peru Basin (34.2% Mn; Wegorzewski and Kuhn, 2014).

Figure 10 compares the results of the bulk-nodule chemical analyses from our work in relation to the results from other parts of CCZ and the Peru Basin by Wegorzewski and Kuhn (2014); the Mn/Fe ratio has no great effect on the Cu and Ni concentrations. Figure 11 compares the average contents of selected elements in nodules from different oceanic areas. Our results from the CCZ are generally similar to those reported for the CCZ, though in the case of Co, Pb, Ba, Y, La, Ce and REY they are slightly lower, while Li and Cu are slightly higher compared to the average levels given by Hein et al. (2013). In general CCZ polymetallic nodules compared to nodules from the Indian

Table 3

Analysis of chemical composition of high-reflectivity and low-reflectivity polymetallic nodules layers based on EMPA data (wt.%)

	Zn	Cu	Ni	Co	Fe	Mn	Na	Si	Al	K	Cl	S	P	Sr	Ba	Mg	Ca	O	Total	Mn/Fe	Ni+Cu
All layers [wt.%]																					
average	0.2	1.7	1.99	0.16	2.37	42.14	1.48	2.31	1.38	0.86	0.2	0.04	0.05	0.05	0.38	2.22	1.42	33.32	92.25	61.79	3.69
min	0.01	0.32	0.18	0.01	0.04	17.1	0.4	0.2	0.15	0.26	0.1	0.01	0.02	0	0.02	0.68	0.58	17.15	65.18	1	0.59
max	0.52	2.75	2.18	0.47	17.85	52.72	2.29	17.89	2.16	1.59	1.05	0.13	0.13	0.13	1.11	3.06	2.63	36.91	100	1148.8	6.43
Type 1, high-reflectivity, bright layers																					
average	0.22	1.92	2.27	0.14	0.86	44.81	1.53	1.92	1.42	0.91	0.15	0.03	0.03	0.05	0.38	2.46	1.23	34.03	94.37	75.62	4.19
min	0.01	0.47	0.36	0.01	0.04	25.94	0.69	0.2	0.15	0.48	0.33	0.03	0.02	0.02	0.72	0.9	0.58	17.15	65.18	5.5	0.83
max	0.52	2.75	4.13	0.47	7.38	52.72	1.22	3.04	2.03	0.92	0.07	0.04	0.06	0.5	0.48	3.06	1.28	36.91	100	1148.8	6.43
Type 2, Low-reflectivity, dark layers																					
average	0.09	0.77	0.82	0.25	8.7	30.9	1.23	3.93	1.23	0.61	0.42	0.07	0.06	0.06	0.38	1.23	2.19	30.32	83.36	3.76	1.58
min	0.02	0.32	0.18	0.1	5.69	17.1	0.4	0.99	0.36	0.26	0.1	0.01	0.02	0	0.02	0.63	0.69	22.89	64.1	1	0.59
max	0.38	1.73	2.18	0.33	17.85	42.55	2.29	17.98	2.16	1.59	1.05	0.13	0.13	0.13	1.11	2.48	2.63	36.43	97.23	5	3.43

All layers – 245, Type 1 – 192, Type 2 – 53

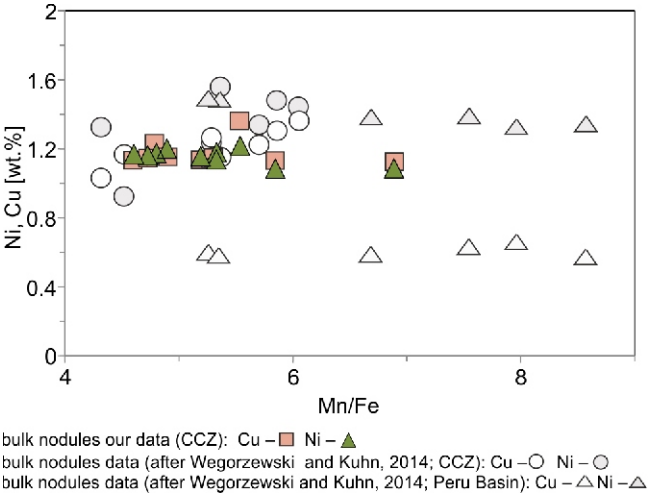

Fig. 10. Comparison of Mn/Fe vs. Ni and Cu contents of bulk polymetallic nodules from our study with other data from the CCZ and from the Peru Basin in the Pacific Ocean (after Wegorzewski and Kuhn, 2014)

Ocean have similar concentrations of Mn, Fe, sum of Co + Cu + Ni, Zn, Mo and V, and much lower, in the case of Pb, Sc, Y, La, Ce and REY but higher for Co and Li. In nodules from the Peru Basin there are also much lower concentrations of Co, Pb, La, Ce and REY than in the CCZ nodules. In the Cook Island nodules, much lower concentrations of Cu, Ni, Zn, Mo, Li and Ba are observable, but higher levels of Co, Pb, As, Y, La, Ce and REY. In nodules from the Gulf of Cadiz and from the southern part of the Baltic Sea, metal concentrations are much lower, at the level of tens to hundreds of ppm. It is characteristic that for the nodules with the lowest Cu and Ni contents (Baltic Sea and Gulf of Cadiz) the highest average Fe concentrations and the lowest Mn contents are found. The mean Mn/Fe ratio in the nodules we investigated (= 5.3) is higher than that reported for CCZ (= 4.6) by Hein et al. (2013). Compared to other areas, the mean Mn/Fe ratios in the nodules vary from 5.58 for the Peru Basin to 0.16 for the Gulf of Cadiz (Fig. 12). The Th/U ratio for the samples we examined, at 3.3, is similar to other data from the CCZ (= 3.6; Hein et al., 2013). Comparison with other areas shows that similar values are characteristic of nodules from the Cook Island EFZ, while significantly lower valyes occur in nodules from the Peru Basin (= 1.6), the Gulf of Cadiz (= 1) and the Baltic Sea (= 0.7).

Comparing the metal content of deep sea deposits with land resources, they may become of great importance in the future at the time of depletion of onshore resources (e.g., Morgan, 2000; Kotliński et al., 2008; Kotliński, 2011; Hein et al., 2013, 2015). Figure 13 shows the median values of bulk rock geochemistry studies of nodules from the CCZ and Kupferschiefer deposits in Poland for comparison. Much higher contents in nodules were found for such elements as Mn, Ni, Co, Mo, Ce, Tl, La, Y, Sb, Cd and As. Moreover, from the Kupferschiefer deposits, critical elements continue not to be recovered in due to the economic unprofitability of their extraction and the lack of appropriate technologies.

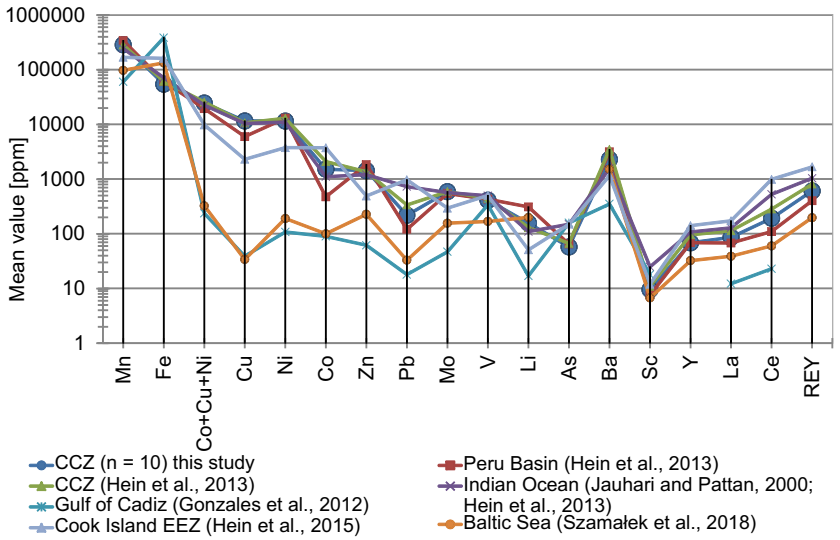

Fig. 11. Comparison of mean value (in ppm) for selected elements (in ppm) in nodules from different parts of the world (data after various authors)

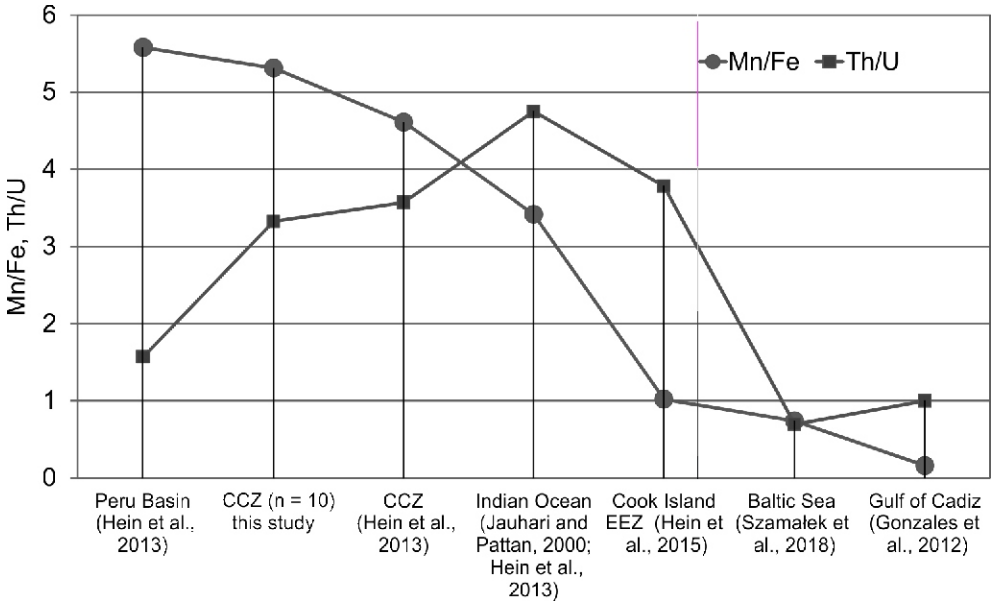

Fig. 12. Comparison of mean values of Mn/Fe and Th/U ratios in nodules from different parts of the world (data after various authors)

The chemical composition of nodules is controlled by several factors such as the type of formation (diagenetic, hydrogenetic and/or mixed type), the geographic location and water depth, growth rate as well as source of metals or local exchange between oxic and anoxic conditions (Koschinsky and Hein, 2003; Hein et al., 2013; Kuhn et al., 2017). The results of our geochemical studies allowed determination not only of the chemical composition of polymetallic nodules from the CCZ in the Pacific Ocean but also their genesis. Values of Mn/Fe ratio 5 in polymetallic nodules are characteristic of a hydrogenetic origin, and values of Mn/Fe ratio 5 for diagenetic ones (Halbach et al., 1988). Furthermore, hydrogenetic nodules have high contents of high field strength elements such as Ti, REY, Zr, Nb, Ta, Hf as well as Co, Ce and Te (Koschinsky and Hein, 2003). A good example of hydrogenetic origin nodules are those from the Cook Islands EEZ in the Pacific Ocean. Diagenetic origin nodules are enriched in Ni, Cu, Ba, Zn, Mo, Li and Ga (von Stackelberg, 2000). Typical example of diagenetic nodules are those from the Peru Basin, though they have lower Cu contents due to more efficient Cu recycling in carbonate sediments as compared to the siliceous sediments of the CCZ (Wegorzewski and Kuhn, 2014). The geochemistry of our polymetallic nodules are characteristic of a mixed diagenetic and hydrogenetic origin, which is a characteristic feature of nodules from the CCZ (Wegorzewski and Kuhn, 2014, with references therein). Indian Ocean nodules from the central part of the basin are relatively rich in Mn, Ni and Cu and are of diagenetic or mixed type, while nodules from the southern part are rich in Fe and Co and are hydrogenetic in origin (Jauhari and Pattan, 2000). However, nodules from the Central Indian Ocean Basin generally show lower metal contents in comparison with nodules from the CCZ (Hein et al., 2013). Nodules

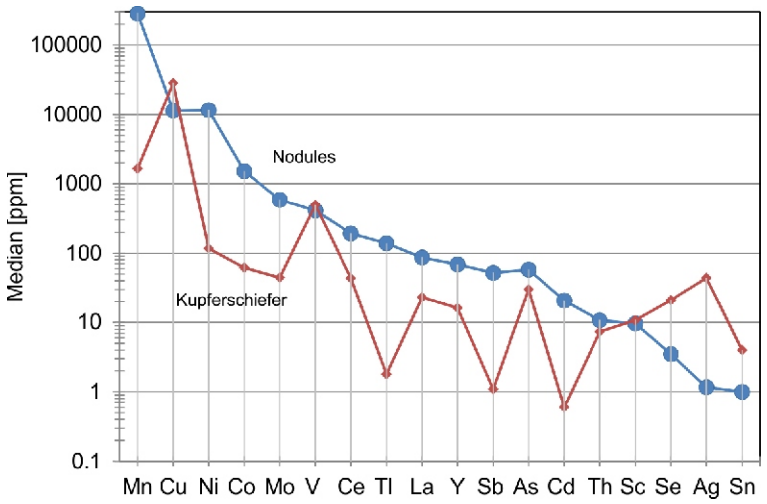

Fig. 13. Comparison of the median content of selected elements in bulk-rock samples of polymetallic nodules from the CCZ in the Pacific Ocean (blue) relative to median contents in the bulk-rock samples of the Kupferschiefer (red) world-class deposits in Poland (after Mikulski et al., 2020)

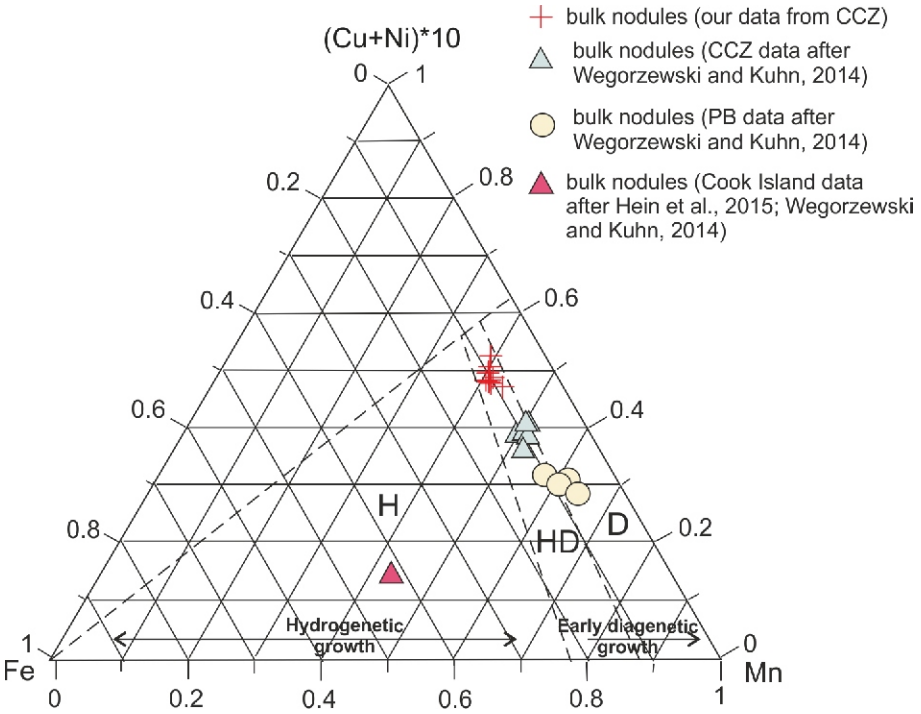

Fig. 14. A ternary diagram of Fe-Mn-(Ni + Cu)*10 according to Bonatti et al. (1972) with data from Wegorzewski and Kuhn (2014) and Hein et al. (2015) showing the bulk-nodule results and relationship between different genetic types of nodules

from the research area have a mixed genesis between hydrogenetic (H) and diagenetic (D). The ratio of manganese to iron is characteristic, with an arithmetic mean of 5.3 (n = 10; range from 4.6 to 6.9). The values of the Mn/Fe ratio are typical for mixed type polymetallic nodules (HD) between the hydrogenetic types that grow on the surface of the sediment in an oxidizing environment and the diagenetic type forming in the bottom sediment. Our geochemical studies of polymetallic nodules from the CCZ zone are consistent with previous studies (e.g., Kotliński, 2011; Abramowski and Kotliński, 2011; Zawadzki et al., 2015). On the ternary diagram after Bonatti et al. (1972) they have similar positions between the fields of hydrogenetic and early diagenetic growth (Fig. 14).

On the diagram after Bau et al. (2014) the nodules studied are classified as of mixed type, e.g. diagenetic and hydrogenetic (Fig. 15A, B).

Moreover, the nodules studied show no Ce anomaly which is also a typical feature of eastern CCZ mixed-origin nodules (Hein et al., 2013). As regards rare earth elements, nodules from the CCZ contain almost 4 times more REY than e.g. Baltic

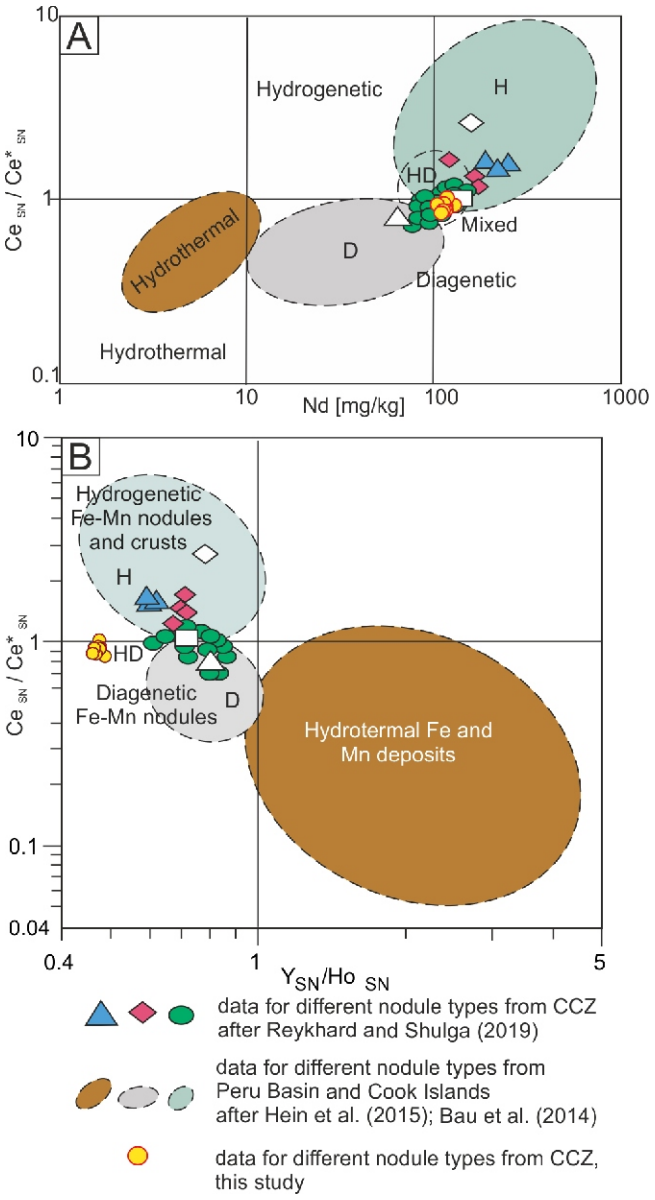

Fig. 15. Diagrams for the determination of the origin of different genetic types of marine Fe-Mn (oxyhydr)oxide nodules after Bau et al. (2014) with our polymetallic nodule samples from the CCZ zone marked as well as other nodules from the CZZ, Peru Basin and Cook Island after various authors

A – Ce_{SN}/Ce_{SN^*} ratios vs. Nd concentration; **B** – Ce_{SN}/Ce_{SN^*} ratio vs. Y_{SN}/Ho_{SN} ratio

nodules (620 ppm/165 ppm). Figure 16 shows the shale (PAAS)-normalized (after McLennan, 1989) rare earth element and yttrium contents of these nodules from CCZ indicating for their mixed origin between the diagenetic and hydrogenetic end members after Kuhn et al. (2017).

The results of our geochemical studies as regards the genesis of the nodules are consistent with the EPMA studies. On their basis, it was found that laminae are different in chemical composition, density, growth structures and reflectivity which makes it possible to assess by which processes (hydrogenetic or diagenetic) their formation took place. According to Koschinsky and Hein (2003), Hein et al. (2013), Wegorzewski and Kuhn (2014), Kuhn et al. (2017), the hydrogenetic layers have a Mn/Fe ratio >5 and increased contents of Ti, Zr, Nb, Co and Te. Growth of hydrogenetic nodules is a very slow process at ~1 to 10 mm per million years (Hein and Petersen, 2013). Laminae formed as a result of diagenesis in anoxic conditions grow at rates of up to a hundred mm per million years (Hein and Petersen, 2013) and have Mn/Fe ratios >5 and higher Ni, Cu, Zn, Mo and Li values. In the case of the nodules investigated, it was observed that the laminae formed as a result of hydrogenesis had increased values of Co, Si, Cl, S and were also rich in Fe and Ca and depleted in Mn, Cu, and Ni. These features indicated that they arose as a result of precipitation from oxidizing seawater (Koschinsky and Halbach, 1995; Koschinsky and Hein, 2003; Wegorzewski and Kuhn, 2014; Kuhn et al., 2017; Wegorzewski et al., 2020). Hydrogenetic growth occurs at the water-sediment interface, where metals and other ions are absorbed directly from oxic seawater. The structure of the surface of the nodules formed by hydrogenetic means is smooth, dense and there is less sediment on the surface.. Laminae formed as a result of diagenesis had increased levels Cu, Ni, Mg, Zn, Al, Na and K. These metal contents as well as Mn/Fe >5 indicate formation under diagenetic conditions. Diagenetic nodules, rich in Mn, Cu and Ni with a relatively lower content of Fe and Co are formed by metal supply metals from suboxic water through the pores of the sediment. The surface structure of diagenetic nodules is rough (Halbach et al., 1988; Beiersdorf, 2009). As noted by Mewes (2014) and Benites et al. (2018), the layers formed in diagenetic processes also form under suboxic conditions. This is characteristic of the nodules from the CCZ area.

Our results suggest that polymetallic nodules from the research area investigated are most often a mixed type, between diagenetic and hydrogenetic, although there are also nodules resulting only from diagenesis. Thus, from 245 EMPA measurements of the chemical compositions of layers, only 53 showed features characteristic of hydrogenetic growth. Figure 17 shows that our EPMA results of polymetallic nodule samples from the CCZ are very similar to the results of Wegorzewski and Kuhn (2014). Low-reflectivity layers (type 2) are characterized by a low content of the sum of Ni and Cu and the Mn/Fe ratio does not exceed 5. In the case of high-reflectivity layers (type 1), the content of Ni and Cu is much higher, but there are also layers with lower amounts of the sum of these elements.

The genetic type of polymetallic nodules can also be assessed macroscopically, taking into account the location of the carbonate compensation depth (CCD). According to Kotliński (1999), hydrogenetic, smaller smoother nodules occur more often above and at the limit of the CCD, while diagenetic, larger and rougher nodules form below the CCD. Differences in the sizes of the polymetallic nodules reflect their structural features associated with different growth rates (Halbach et al., 1981, 1988; Kotliński, 1999). Many polymetallic nodules, especially large ones, show characteristic features of diagenetic growth where the nodules are in contact with sediment and hydrogenetic growth at the place of direct contact with water. Despite the characteristic macroscopic appearance of the nodule types, their internal structure and metal content may indicate a mixed origin.

CONCLUSIONS

1. The nodules studied from the Clarion-Clipperton Fracture Zone in the Pacific Ocean are from 3.3 to 7.6 cm across and discoidal to ellipsoidal in shape, usually with a smooth upper surface and rough bottom parts. They have a characteristic

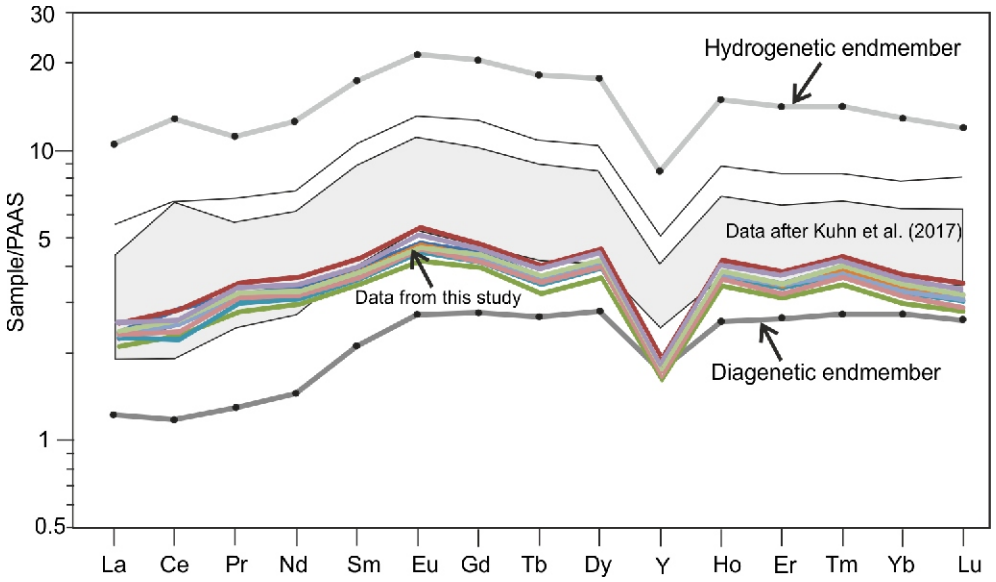

Fig. 16. Shale (PAAS)-normalized (after McLennan, 1989) rare earth element and yttrium contents (REY) of nodules from the CCZ indicating for their mixed origin between the diagenetic and hydrogenetic end members (after Kuhn et al., 2017)

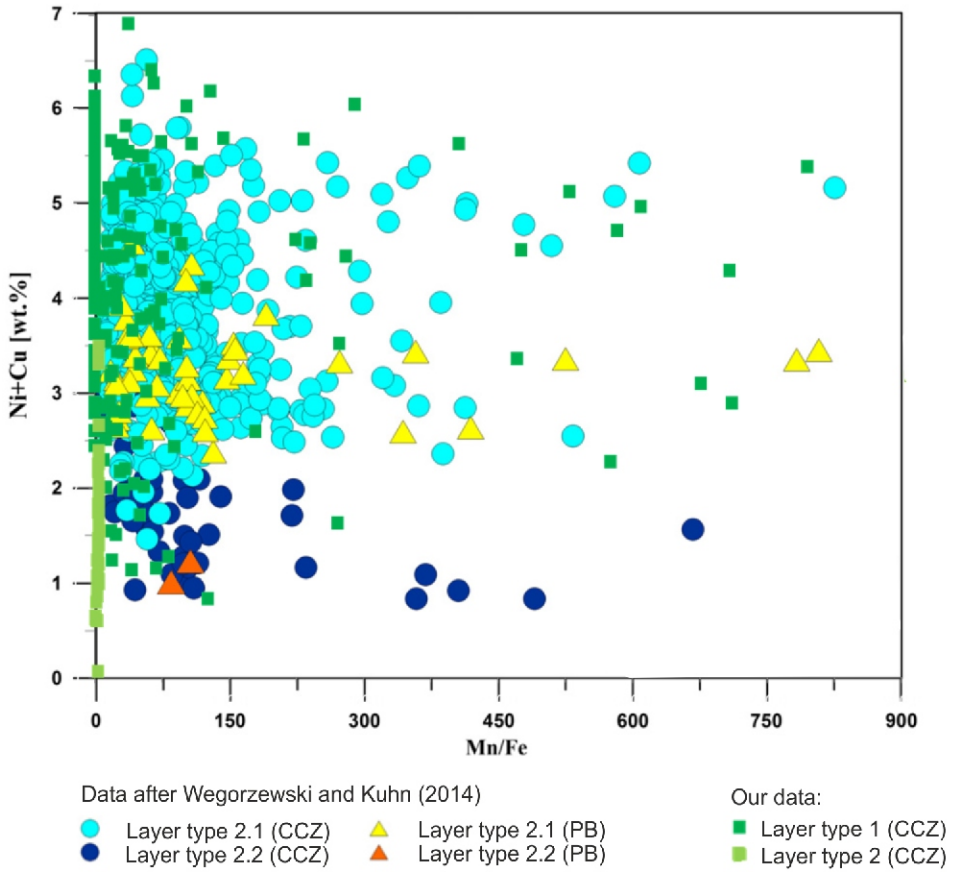

Fig. 17. Ni +Cu vs. Mn/Fe ratios of type 2 layers of nodules from the CCZ and Peru Basin after Wegorzewski and Kuhn (2014) compared with our EPMA results of polymetallic nodule samples from the CCZ

concentric structure in which thin laminae (1 to 2 mm thick) of Mn-Fe (oxyhydr)oxide crystallize around a foreign nucleus. EPMA revealed that two types of layer can be distinguished, which differ in shape, thickness and reflectivity that is indicative of different element contents. High-reflectivity layers are thicker then low-reflectivity layers. They are porous and rounded and usually grow in dendritic or massive forms. Massive parts are dense and thick and often containing numerous visible fragments of microfauna such as radiolaria and diatoms that may have grown within the pore space of the sediments. This type of lamina contains a high value of Mn (mean 44.8 wt.%), low Fe content (0.86 wt.%) and concentration of Ni+Cu (up to 6.4 wt.%). The Mn/Fe ratio ranges from 5.5 to 1148.8. This type of layer is very common and covers a large area of the inner nodule structure. Low-reflectivity layers usually grow in the form of fine lamination but also in a dendritic form, commonly creating an mixed sequence, in alternating with light layers. They contain significant amounts of Fe (5.7–17.9 wt.%) and of silica (in average 3.93 wt.%). The Mn/Fe ratio ranges from 1 to 5 and the concentration of Ni+Cu is relatively low (up to 3.43 wt.%).

2. The bulk-nodule geochemical studies (ICP-MS, WD-XRF and GFAAS) from the CCZ showed that they are built mainly of MnO (35.8–39.5 %), SiO_2 (12.2–13.7 %), Fe_2O_3 (6.3–8.8%) and Al_2O_3 (4.1–4.7%). They have strong enrichment in Cu (1.1–1.4%), Ni (1.1–1.2%), Ba (1472–3965 ppm), Co (1297–1711ppm), Zn (1263–1683 ppm), Mo (518–672 ppm), V (381–447 ppm), Pb (193–251 ppm), Li (118–203 ppm) and REY (553.6–677.4 ppm). The polymetallic nodules from the CCZ are much richer in some elements (Cu, Ni, Zn, Mo, Ba and REY) than nodules from other areas (e.g. Cook Island EFZ, Gulf of Cadiz and Baltic Sea). The nodules from the Peru basin have a higher average contents of Ni, Zn, Li and Ba but much lower Cu and Co concentrations when compared with our data from CCZ.

3. The bulk-nodule ratio of Mn/Fe is in the range 4.6–6.9 (mean = 5.3) and is characteristic of nodules of mixed origin consisting of hydrogenetic and diagenetic growth structures. Moreover, their mixed origin is consistent with the positions of our samples on the discriminant diagrams of Bonatti et al. (1972) and Bau et al. (2004). Furthermore, the characteristic REY pattern of the shale (PAAS after McLennan, 1989)-normalized nodules from the CCZ also indicate their mixed origin between the diagenetic and hydrogenetic end members (after Kuhn et al., 2017).

Acknowledgements. We are very grateful to the InterOceanMetal Joint Organization for providing the Polish Geological Institute – National Research Institute with samples of polymetallic nodules from the CCZ in the Pacific Ocean. This work is financially supported by the Polish Geological Institute-National Research Institute through internal grant no. 61.6199.1601.00.0 for SM.

REFERENCES

Abramowski, T., Kotliński, R.A., 2011. Contemporary challenges in exploitation of the ocean polymetallic deposits (in Polish with English summary). Górnictwo i Geoinżynieria, **35**: 41–61.

Barbalance, K., 2019. Periodic Table of Elements. Available online: environmental chemistry.com

Baturin, G.N., 1988. The Geochemistry of Manganese and Manganese Nodules in the Ocean. Springer, Dordrecht.

Bau, M., Schmidt, K., Koschinsky, A., Hein, J., Kuhn, T., Usui, A., 2014. Discriminating between different genetic types of marine ferro-manganese crusts and nodules based on rare earth elements and yttrium. Chemical Geology, **381**: 1–9.

Beiersdorf, H., 2009. Scientific challenges related to the development of a geological model for manganese nodule occurrences in the Clarion-Clipperton zone (Equatorial North Pacific Ocean). Proceedings of the International Seabed Authority's Workshop, Nadi, Fiji, 2003 ISA, Kingston, Jamaica: 175–201.

Benites, M., Millo, Ch., Hein, J., Nath B.N., Murton, B, Galante, D., Jovane, L., 2018. Integrated geochemical and morphological data provide insights into the genesis of ferromanganese nodules. Minerals, **8** (11).

Bonatti, E., Kraemer, T., Rydell, H., 1972. Ferromanganese deposits on the ocean floor. Washington Natural Science Foundation: 149–166.

Cronan, D.S., 1977. Deep Sea Manganese Nodules: Distribution and Geochemistry. In: Marine Manganese Deposits (ed. G.P. Glasby): 11–44. Elsevier, Amsterdam.

Depowski, S., Kotliński, R., Rühle, E., Szamałek, K., 1998. Surowce mineralne mórz i oceanów (in Polish). Wydawnictwo Naukowe Scholar, Warszawa.

Dimitrina, D., Milakovska, Z., Peytcheva, I., Stefanova, E., Stoyanova, V., Abramowski, T., Walle, M. 2014. Trace element and REY composition of polymetallic nodules from the easternClarion-Clipperton Zone (Northern Pacific Ocean) determined by in situ LA-ICP-MS analyses. Comptes rendus de l'Academie bulgare des Sciences, **67**: 267–274.

Duliu, O.G., Alexe, V., Moutte, J., Szobotca, S.A. 2009. Major and trace element distribution in manganese nodules as well as abyssal clay from the Clarion-Clipperton abysal plain, Northern Pacific. Geo-Marine Letters, **29**: 71–83

Franzen, J., Balaz, P. 2012. Rare earth elements in the polymetallic nodules – a new challenge. Proceeding of the 23rd International Offshore and Polar Engineering Conference, Rhodes, Greece, 17–22 June: 112–116.

Glasby, G.P., 1977. Marine Manganese Deposits. Elsevier, Amsterdam.

Glasby, G.P., 2006. Manganese: predominant role of nodules and crusts. In: Marine Geochemistry: 371–428. Springer, Heidelberg.

Gonzalez, F.J., Somoza, L., Lunar, R., Martinez-Frias, J., MartinRubi, J.A., Torres, T., Ortiz J.E., Diaz-del-Rio, V., 2012. Internal features, mineralogy and geochemistry of ferromanganese nodules from the Gulf of Cadiz: the role of the Mediterranean Outflow Water undercurrent. Journal of Marine Systems, **80**: 203–218.

Gordon, R., 2000. Diffuse oceanic plate boundaries: strain-rates, vertically averaged rheology and comparisons with narrow plate boundaries and stable plate interiors. Geophysical Monograph Series, **121**: 143–159.

Halbach, P., Scherhag C., Hebisch, U., Marchig, V., 1981. Geochemical and mineralogical control of different genetic types of deep-sea nodules from the Pacific Ocean. Mineralium Deposita, **16**: 59–84.

Halbach, P., Friedrich, G., von Stackelber, U., 1988. The Manganese Nodule Belt of the Pacific Ocean. Geological Environment, Nodule Formation and Mining Aspects. Ferdinand Enke Verlag, Stuttgart, Germany.

Hein, J., 2000. Cobalt-rich Ferromanganese Crusts: Global Distribution, Composition, Origin and Research Activities, Polymetallic Massive Sulphides and Cobalt-Rich Ferromanganese Crusts: Status and Prospects. International Seabed Authority, Kingston, Jamaica.

Hein, J.R., Koshinsky, A., 2014. Deep-ocean ferromanganese crusts and nodules. The Treatise on Geochemistry **12:** 273–291.

Hein, J.R., Petersen, S., 2013. The geology of manganese nodules. Deep Sea Minerals: Manganese Nodules. A Physical, Biological, Environmental and Technical Review, **1**: 7–18.

Hein, J.R., Koshinsky, A., Halbach, P., Manheim, F.T., Bau, M., Kang, J.K., Lubick, N., 1997. Iron and manganese oxide mineralization in the Pacific. Geological Society Special Publications, **119**: 123–139.

Hein, J.R., Mizell, K., Koschinsky, A., Conrad, T.A., 2013. Deep-ocean mineral deposits as a source of critical metals for high- and green-technology applications: comparison with land-based resources. Ore Geology Reviews, **51**: 1–14.

Hein, J.R., Spinardi, F., Okamoto, N., Mizell, K., Thorburn, D., Tawake, A., 2015. Critical metals in manganese nodules from the Cook Islands EEZ, abundances and distributions. Ore Geology Reviews, **68**: 97–116.

Jauhari, P., Pattan, J.N., 2000. Ferromanganese deposits in the Indian Ocean. In: Handbook of Marine Mineral Deposits (ed. D.S. Cronan): 171–195. CRC Publications, NY.

Kazmin, Y., 2009. Relationship between nodule grade and abundance and tectonic and volcanic activity in the Clarion-Clipperton Zone. Proceedings of the International Seabed Authority's Workshop held 2003 in Nadi, Fiji, International Seabed Authority, Kingston, Jamaica: 145–160.

Koschinsky, A., Halbach, P., 1995. Sequential leaching of marine ferromanganese precipitates: genetic implications. Geochimica et Cosmochimica Acta, **59**: 5113–5132.

Koschinsky, A., Hein, J.R., 2003. Uptake of elements from seawater by ferromanganese crust: solid phase association and seawater speciation. Marine Geology, **198**: 331–351.

Kotliński, R., 1992. Results of geological and exploration studies of polymetallic nodules in the Clarion-Clipperton zone in the Pacific Ocean (in Polish with English summary). Przegląd Geologiczny, **40**: 253–260.

Kotliński, R., 1999. Metallogenesis of the World's ocean against the background of oceanic crust evolution. Polish Geological Institute Special Papers, **4**.

Kotliński, R., 2011. Pole konkrecjonośne Clarion-Clipperton – źródło surowców w przyszłości (in Polish). Górnictwo i Geoinżynieria, **35**: 195–214.

Kotliński, R., Stoyanova V., 2005. Control factors of polymetallic nodules distribution within the Eastern area of the Clarion-Clipperton Zone (CCZ). VI ISOPE Ocean Mining Symposium, Changsha, Chiny, 9–13 October: 1–11.

Kotliński, R., Parizek, A., Rezek. K., 1997. Polymetallic nodules – a possible source of Rare Earth Elements. The Proceedings of the 2nd ISOPE Ocean Mining Symposium, Seoul, Korea: 50–56.

Kotliński, R., Mucha J., Wasilewska, M., 2008. Metodyka szacowania parametrów zasobowych złóż konkrecji polimetalicznych w obszarze Interoceanmetal na Pacyfiku (in Polish). Gospodarka Surowcami Mineralnymi. **24**: 257–266.

Kozłowska-Roman, A., Mikulski, S.Z., 2019. Morphological and mineralogical characteristics of polymetallic nodules from the Clarion-Clipperton zone on the Pacific Ocean – preliminary results (in Polish with English summary). Przegląd Geologiczny, **67**: 169–172.

Kuhn,T., Wegorzewski, A., Rühlemann, C., Vink A., 2017. Composition, Formation, and Occurrence of Polymetallic Nodules. In: Deep-Sea Mining Resource Potential, Technical and Environmental Considerations (ed. R. Sharma): 23–64. Springer, Berlin/Heidelberg.

McLennan, S.M., 1989. Rare earth elements in sedimentary rocks: influence of provenance and sedimentary processes. Reviews in Mineralogy, **21**: 169–200.

Mewes, K., Mogollón, J.M., Picard, A., Rühlemann, C., Kuhn, T., Nöthen, K., Kasten, S., 2014. Impact of depositional and biogeochemical processes on small scale variations in nodule abundance in the Clarion-Clipperton Fracture Zone. Deep-Sea Research, **91**: 125–141.

Mikulski, S.Z., Oszczepalski, S., Sadłowska, K., Chmielewski, A., Małek, R., 2020. Trace element distributions in the Zn-Pb (Mississippi Valley-Type) and Cu-Ag (Kupferschiefer) sediment-hosted deposits in Poland. Minerals, **10**: 75.

Morgan, Ch.L., 2000. Resources estimates of the Clarion-Clipperton manganese nodule deposits. In: Handbook of Marine Mineral Deposits (ed. D.S. Cronan): 145–170. CRC Publications, NY.

Mukhopadhyay, R., Ghosh, A.K., Iyer, S.D., 2018. The Indian Ocean Nodule Field. Geology and Resource Potential. Elsevier, 2nd edition.

Neall, V., 2008. Review – The age and origin of the Pacific islands: a geological overview. Philosophical Transactions of The Royal Society B Biological Sciences, **363**: 3293–3308.

Rona, P.A., 2008. The changing vision of marine minerals. Ore Geology Reviews, **33**: 618–666.

Ruhlemann, C., Kuhn, T., Kasten, S., Mewes, K., 2011. Current status of manganese nodule exploration in the German license area. Proceedings of the Ninth, ISOPE Ocean Mining Symposium, Hawaii.

Szamałek, K., Uścinowicz, Sz., Zglinicki K., 2018. Rare earth elements in Fe-Mn nodules from southern Baltic Sea – a preliminary study. Biuletyn Państwowego Instytutu Geologicznego, **472**: 199–212.

Usui, A., Someya, M., 1997. Distribution and composition of marine hydrogenetic and hydrothermal manganese deposits in the northwest Pacific. Geological Society Special Publications, **119**: 177–198.

Wegorzewski, A., Kuhn, T., 2014. The influence of suboxic diagenesis on the formation of manganese nodules in the Clarion Clipperton nodule belt of the Pacific Ocean. Marine Geology, **357**: 123–138.

Wegorzewski, A.V., Kuhn, T., Dohrmann, R., Wirth, R., Grangeon, S., 2015. Mineralogical characterization of individual growth structures of Mn-nodules with different Ni+Cu content from the central Pacific Ocean. American Mineralogist, **100**: 497–2508.

Wegorzewski, A.V., Grangeon, S., Webb, S.M., Heller, C., Kuhn, T., 2020. Mineralogical transformations in polymetallic nodules and the change of Ni, Cu and Co crystal-chemistry upon burial in sediments. Geochimica et Cosmochimica Acta, **282**: 19–37.

von Stackelberg, U., 2000. Manganese Nodules of the Peru Basin. In: Handbook of Marine Mineral Deposits (ed. D.S. Cronan): 197–238. CRC Publications, NY.

von Stackelberg, U., Beiersdorf, H.,1991. The formation of manganese nodules between the Clarion and Clipperton Fracture-Zones south east of Hawaii. Marine Geology, **98**: 411–423.

Yubko, V.M., 2009. Regional and local trends in the formation of polymetallic nodule deposits in the Clarion-Clipperton Zone. Proceedings of the International Seabed Authority's Workshop held 2003 in Nadi, Fiji, International Seabed Authority, Kingston, Jamaica: 222–232.

Yubko, V.M., Kotliński, R., 2009. Volcanic, tectonic and sedimentary factors. In: Prospector's Guide for Polymetallic Nodule Deposits in the Clarion-Clipperton Fracure Zone (ed. Ch.L. Morgan): 4–30. Kingston, Jamaica.

Zawadzki, D., Maciąg, Ł., Kotliński, R.A., 2015. Eupelagic sediments as a potential resource for rare earth elements (in Polish with English summary). Biuletyn Państwowego Instytutu Geologicznego, **465**: 131–142.

Zawadzki, D., Maciąg, Ł., Abramowski, T., Mc Cartney, K,. 2020. Fractionation trends and variability of Rare Earth Elements and selected critical metals in pelagic sediment from abyssal basin of NE Pacific (Clarion-Clipperton Fracture Zone). Minerals, **10**: 320.